# Theoretical Studies on Electrocompression of Electrodeposited Halide Monolayer on Au(111) Surface

**Xueqin Wang, Rong Chen, Yuliang Wang, Tianjing He, and Fan-Chen Liu***

*Department of Chemical Physics, University of Science and Technology of China, Hefei, Anhui 230026, People's Republic of China*

*Received: January 7, 1998; In Final Form: June 29, 1998*

A simple physical model and theory have been proposed to investigate the electrocompression behavior of electrodeposited halide (chloride, bromide, and iodide) monolayer at the Au(111) electrode surface. By establishing the statistical thermodynamic formulas, the effective pair interaction energy, 2D spreading pressure, 2D isothermal compressibility, and electrode potential-coverage ($\theta$-$E$) curves of halide monolayer at Au(111) surface have been calculated. The theoretical results are in good agreement with the experimental measurements, which show that the adatom−adatom interactions, especially repulsive interactions, determine the size of the compressibility in the halide adlayer on Au(111) surface with an increase in the electrode potential. The electrosorption valency $\gamma$ of halide also plays an important role on the electrocompression. The theory in this paper is in principle applicable to other anion species at metal electrode surface.

## 1. Introduction

The adsorption behavior and adlayer structures of ionic species on a metal electrode surface are important in many fields of science including biology, geology, and electrochemistry. A typical example is the chemical adsorption of chloride, bromide, and iodide. Recently, the electrodeposited monolayer of chloride, bromide, and iodide on Au(111) electrode surface has been studied experimentally by in-situ scanning tunneling microscopy (STM)[1−5] and surface X-ray scattering (SXS).[5−8] These studies have demonstrated that all these three kinds of halide adatoms can form well-ordered structures at Au(111) surface and the structures continuously compress with increasing the electrode potential. The term "electrocompression" was used to describe this phenomenon, which emphasizes the potential-dependent origin of the compression.[7] It is also known[9,10] that this electrocompression is common among electrodeposited metal adlayers. Though the electrocompressive behavior of halide adlayer phases has been successfully studied in the experiments, any theory of this electrocompression in anionic adlayer, even a simple phenomenological model which incorporates the known physical effects, has not exist yet.[5,7,8] The free electron model, which has been used to successfully describe the electrocompression of electrodeposited metal monolayer on Ag(111) surface,[9,10] does not appear to apply for anion adlayers.[7]

In this paper, we attempt to use a simple physical model to investigate the structures and electrocompression of halide monolayer on Au(111) electrode surface. First, statistical thermodynamics formulas for the halide adlayer on Au(111) surface were established. Then the curves of electrode potential versus adsorbate coverage, two-dimensional (2D) isothermal compressibility, adsorbate−adsorbate (lateral) interaction energies, and two-dimensional (2D) spreading pressure in the halide adlayer at Au(111) surface have been calculated and compared with the experimental investigation carried out by Ocko et al.[7,8] Reasonable agreement between theory and experiments is achieved. In the adatom−adatom interactions of this (quasi-) two-dimensional system, the substrate-mediated interaction, electrostatic interaction, Lennard-Jones potential, the induced dipole−induced dipole interaction, and nonadditive three body potential are taken into account. The results show that adatom−adatom interactions are strongly repulsive in all the three halide adlayers, which determine the size of the compressibility in the adlayers on Au(111). Comparing the theoretical calculation with the experimental measurement also shows that the electrosorption valency is very important in the process of electrocompression.

Our model in this paper supplies a method in principle to study the electrochemical behavior of anion species at electrode surface. In subsequent sections, first, we propose a physical model and establish statistical mechanics formulas in section 2, analyze and discuss the adsorbate−adsorbate interaction energies in the adlayer in section 3, and the calculation results are given and discussed in section 4.

## 2. Physical Model and Fundamental Formulas

**2.1. Physical Model and Partition Function.** Our physical model for chloride, bromide and iodide adsorbate monolayers on Au(111) electrode assumes that every adsorbed monolayer consists of a regular two-dimensional lattice of halide adatoms and does not directly include the solvent molecules in the model based on the following experimental facts. (i) It is known[6,11−13] that the electrode interface ions may lose all (in chemisorption) or part of their hydration sheath, specially on condition that the adsorbed ions include anions such as $Cl^-$, $Br^-$, and $I^-$ and metal ions. (ii) The halide adlayer structures in electrochemical systems in aqueous solution are similar to those in vacuum.[1,5] The equivalent in this very different kind of environment indicates that the interaction between the solvent molecules and the adatoms may not influence the halide monolayer structures. (iii) Additionally, water molecules are not found in STM picture of halide adlayer on Au(111) surface.[2] Thus, without considering the solvent molecules, halide ($X^-$) chemisorbed on Au(111)

* Corresponding author. Email: tianjing@dchp.chp.ustc.edu.cn. Fax: +86-0551-3631760.

S1089-5647(98)00699-3 CCC: $15.00 
Published on Web 09/09/1998

electrode can be viewed essentially as a charge-transfer process[4,11−14]

$$X^- (sol) + Au(surf) \leftrightarrow X^{-(1+\gamma)} + Au(surf) - \gamma e \quad (1)$$

where $\gamma$ is the electrosorption valency.

We suppose that the equilibrium positions of adsorbates in the incommensurate halide adlayers on Au(111) can occupy any point on the surface rather than specific sites so that the adsorbates can be compressed uniformly. Each halide adsorbate on Au(111) surface has three vibrational degrees of freedom. In *z*-direction perpendicular to the surface, adsorbate−metal surface stretching vibration with frequency $\nu_z$ can exist, and there are also vibrations in *x*- and *y*-directions around the potential energy minimum with frequencies $\nu_x$ and $\nu_y$. Because no reliable data about the phonon spetctrum of the 2D layer are accessible,[15] here we adopt the Einstein model, which is a good approximation for three-dimensional crystals under the condition that $T > \theta_d$, where $\theta_d$ is Debye temparature and $\theta_d$ = 106 K for iodine.[16,70]

All the adsorbates on the surface can be considered as a canonical ensemble. Because no two- or three-dimensional lattice statistics problem has as yet been given a treatment that is both complete and exact, approximate methods are useful.[17a] In our model, the Bragg−Williams approximation is used, which is generally accepted and widely used in a system of adsorbates at a metal electrode.[18] As Guidelli pointed out[18] that, with only a few exceptions, the monolayer models available in the literature make use of Bragg−Williams approximation. If the number of substrate sites and the number of adsorbates are respectively denoted by $N_S$ and $N_A$, then the partition function (PF) to describe the halide adsorbate monolayer can be written as[16,17b,19]

$$(PF) = \frac{N_S!}{N_A!(N_S - N_A)!} j^{(S)}(T)^{N_A} \exp\left[-\frac{N_A(U+V)}{kT}\right] \quad (2)$$

where $U$ is the potential energy at the minimum in an adatom−substrate interaction energy $U(xyz)$. Then the adsorption energy per atom at 0 K is $U + \sum_{i=x,y,z} h\nu_i/2$. $V$ is an average adatom−adatom interaction energy (the lateral interaction energy) per adatom

$$V = 1/2Z\theta W \quad (3)$$

where $Z$ is the nearest-neighbor (nn) coordinate number of an adsorbate. $\theta = N_A/N_S$ is the coverage of adsorbates relative to the substrate. $W$ in eq 3 is an effective pair interaction energy between adsorbates

$$W = \frac{\sum_j V_{ij}}{Z} \quad (4)$$

where $V_{ij}$ is a pair interaction energy between the adsorbates $i$ and $j$ in the adlayer. The sum in eq 4 is over all lattice sites in the adlayer except the adsorbate $i$. $j^{(S)}$(T) in eq 2 is partition function of a three-dimensional harmonic oscillator with the vibrational frequencies $\nu_x$, $\nu_y$, and $\nu_z$,

$$j^{(S)}(T) = \prod_{i=x,y,z} \frac{e^{h\nu/kT}}{e^{h\nu_i/kt} - 1} \quad (5)$$

From eq 2

$$\ln(PF) = N_S \ln N_S - N_A \ln N_A - (N_S - N_A)\ln(N_S - N_A) + N_A \ln j^{(S)}(T) - \frac{N_A U}{kT} - \frac{Z N_A^2 W}{2 N_S kT} \quad (6)$$

which is similar to eq 14−42 in ref 17b.

Then, the free energy thermodynamics function is obtained as

$$F = -kT\ln(PF) = -kTN_S \ln N_S + kTN_A \ln N_A + kT(N_S - N_A)\ln(N_S - N_A) - kTN_A \ln j^{(S)}(T) + N_A U + \frac{ZN_A\theta W}{2} \quad (7)$$

from which thermodynamics properties of the adlayer can be deduced.

In our physical model, a canonical ensemble is used. For the halide adlayer on Au(111), the halide atoms are constantly exchanging from the surface to the solution, and it seems that a grand canonical ensemble is more suitable. However, it is known[17c] that, due to thermodynamics eqivalence of ensembles, for practical thermodynamic purpose, there is no distinction between a grand canonical ensemble and a canonical ensemble. In a given problem, one can choose between them simply on the basis of mathematical convenience and the results must be independent of the choice.

**2.2. Fundamental Formulas of 2D Spreading Pressure and 2D Isothermal Compressibility.** Analogous to the introduction of the pressure P in three-dimensional phases, one can introduce the two-dimensional (2D) pressure $\varphi$ in surface study.[16,20] From eq 7, the statistical mechanics expression of 2D spreading pressure can be written as[17a]

$$\varphi = -\left(\frac{\partial F}{\partial A}\right)_{N_A,T} = \frac{kT}{a_S}\left(\frac{\partial \ln(PF)}{\partial N_S}\right)_{N_A,T} = \frac{ZW\theta^2}{2a_S} - \frac{kT}{a_S}\ln(1-\theta) + kTN_A \frac{d}{dA}\ln j^{(S)}(T) - N_A \frac{dU}{dA} - \frac{ZN_A\theta}{2}\frac{dW}{dA} \quad (8)$$

Since $a = A/N_A$ is area of a single adsorbate, eq 8 becomes

$$\varphi = \frac{ZW\theta^2}{2a_S} - \frac{kT}{a_S}\ln(1-\theta) + kT\frac{d}{da}\ln j^{(S)}(T) - \frac{dU}{da} - \frac{Z\theta}{2}\frac{dW}{da} \quad (9)$$

The origin of the last term in eq 9 is due to the fact that the effective pair interaction energy $W$ between adsorbates is dependent on separation $r$ between the adsorbates. In the case of electrocompression in the halide adlayer at Au(111) surface, the adlayer unit cell size and $r$ continuously decreasing with an increase of the potential $E$ and coverage $\theta$, thus the quantity $dW/da$ is not zero.[21,22]

Now, the factors $dU/da$, $(d/da)\ln j^{(S)}(T)$ and $dW/da$ in eq 9 are analyzed and discussed respectively as follows. First, we discuss the factor $dU/da$. The assumption $dU/da = 0$ is often used in statistical thermodynamics calculations of the adlayer on the various surfaces,[23−26] which is also the essential results of the lattice gas model.[27] The same assumption, $dU/da \approx 0$, has been used in this paper due to the following reasons. (i) Ocko et al.'s experiments[5,7,8] clearly demonstrated that for the

hexagonal phase and the ($p\times\sqrt{3}$) centered rectangular phase of the halide adlayer on Au(111) there are no changes in the Au−X interlayer separation with an increasing electrode potential and coverage except in the phase transition point. The close relation between covalence bond length and bond energy[28] indicates that Au−X bond energy, i.e., the adsorption energy $U$, does not change with the electrode potential and coverage except in the phase transition point. (ii) Gao and Weaver's SERS experiment[29] shows that in the wide 1−2 V potential ranges the vibration band intensities of halide on Au electrode are roughly constant, the vibrational band frequency shows only a small value of potential dependence $d\nu_i/dE$. It is know[27] that the frequencies of vibrations in adsorbed molecules depend sensitively on the binding sites, and the band intensity of adsorbate at different adsorption sites reflects (or proportional to) the number of adsorbates at the respective binding sites. Hence, from Gao and Weaver's results,[29] one can infer that the adsorption energy $U$ of a halide adsorbate on an Au electrode are roughly constant in the wide potential ranges, as well as in the wide coverage ranges since the coverage changes with increasing potential. (iii) Gao and Weaver et al.'s STM results of the iodide have shown[4] that the average adlayer compressibilities (or the slope of $\Gamma-E$ curve) are very similar on the three faces Au(111), (110), and (100). This observation of closely similar, even nearly identical compressibilities on the three low-index faces, indicates that the average adlayer compressibilities are not sensitive to the adsorbate sites on Au, and thus not to the adsorption energy $U$. More directly, nearly equal adsorption free energies obtained experimentally by Van Huong et al.[30] for bromide at (111), (100), (110), and (311) single crystals of gold, which are 120, 123, 122, and 128 kJ/mol, respectively, further supports this assumption.

Second, we consider the factor $(d/da)\ln j^S(T)$ in eq 9. According to eq 5, we have

$$\mathrm{d}/\mathrm{d}a \ln j^{(S)}(T) = \prod_{i=x,y,z} f(\nu_i,T)\frac{\mathrm{d}\nu_i}{\mathrm{d}a} \tag{10}$$

where $f(\nu_i,T)$ is a function of band frequency $\nu_i$ and temperature $T$. Gao and Weaver's SERS results[29] show that the frequency $\nu_i$ is nearly constant in the wide potential and coverage ranges, i.e., $d\nu_i/dE \approx 0$, $d\nu_i/da \approx 0$, implying $\mathrm{d}/\mathrm{d}a \ln j^{(S)}(T) \approx 0$.

Finally, we consider the factor $dW/da$ in eq 9. Since $\theta = a_S/a$, thus,

$$\frac{\mathrm{d}W}{\mathrm{d}a} = -\frac{a_S}{a^2}\frac{\mathrm{d}W}{\mathrm{d}\theta} = -\frac{\theta^2}{a_S}\frac{\mathrm{d}W}{\mathrm{d}\theta} \tag{11}$$

Putting $dU/da = 0$, $\mathrm{d}/\mathrm{d}a \ln j^{(S)}(T) = 0$, and eq 11 into eq 9, we obtain

$$\varphi = \frac{ZW\theta^2}{2a_S} - \frac{kT}{a_S}\ln(1-\theta) + \frac{Z\theta^3}{2a_S}\frac{\mathrm{d}W}{\mathrm{d}\theta} \tag{12}$$

This is a fundamental formula of the 2D spreading pressure. It is evident that the 2D spreading pressure is determined by two factors: adsorbate density and the adatom−adatom interaction with its derivative. The remaining problem is to obtain the relation between the effective pair interaction energy $W$ and the adsorbate coverage $\theta$.

Usually a pair interaction energy $V_{ij}$ between the adsorbates $i$ and $j$ in eq 4 can be written as a sum of the inverse power of the distance $r_{ij}$,

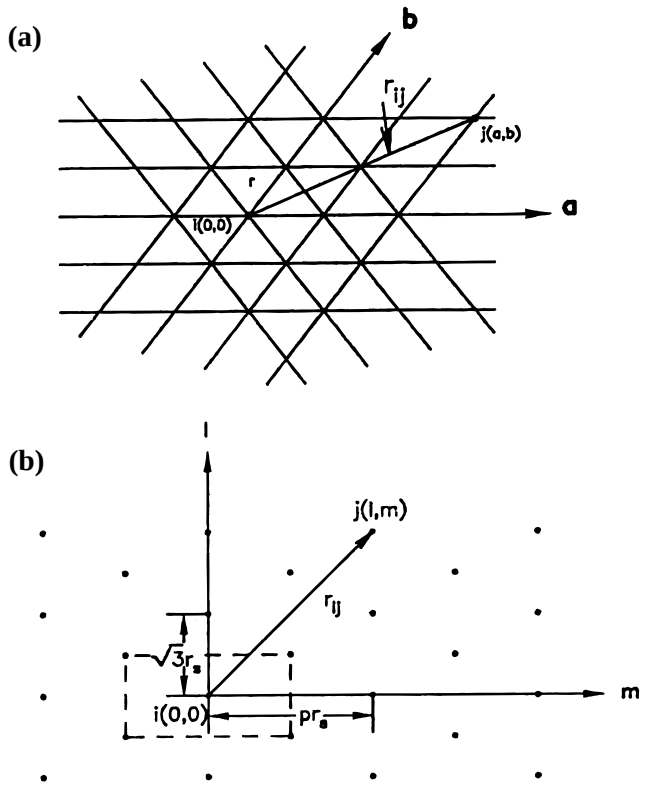


**Figure 1.** (a) The hexagonal network in the halide adlayer (b) The ($p\times\sqrt{3}$) centered rectangular network in the iodide adlayer

$$V_{ij} = \sum_n \frac{C_n}{r_{ij}^{\,n}} \tag{13}$$

then the effective pair interaction energy $W$ is

$$W = \sum_n \frac{C_n}{Z}\sum_j \frac{1}{r_{ij}^{\,n}} \tag{14}$$

where the summation in eq 14 is dependent on the adlayer structure.

The experiment results indicate[7,8] that all the three halide adlayer on Au(111) show the hexagonal structure (see Figure 1a) in certain potential ranges, and iodide monolayer also shows a ($p\times\sqrt{3}$) centered rectangular structure (see Figure 1b) where $p = 1/\theta$.[7] For simplicity, we only study the hexagonal structure here and leave the ($p\times\sqrt{3}$) rectangular phase in Supporting Information.

Based on Figure 1a, the sum over $j$ in eq 14 can be calculated as[31]

$$\sum_j \frac{1}{r_{ij}^{\,n}} = \frac{A_n}{r^n} \tag{15}$$

and

$$A_n = 6\sum_{a=1}^{\infty}\sum_{b=0}^{\infty}(a^2+ab+b^2)^{-n/2} \tag{16}$$

where $a$ and $b$ are coordinates of an adatom $j$, $r$ is the nearest-neighbor distance between adsorbates in the adlayer, and $A_n$ is the lattice sum.

Because $a_S = \sqrt{3}r_S^2/2$ in Au(111) surface and $a = \sqrt{3}r^2/2$ in the halide hexagonal adlayer, eq 15 becomes

$$\sum_j \frac{1}{r_{ij}^{\,n}} = \frac{A_n}{r_S^{\,n}}\theta^{n/2} \tag{17}$$

Thus, by using eqs 14 and 17, $W$ becomes

$$W = \sum_n W_n$$

$$W_n = \frac{A_n}{Z}\frac{C_n}{r^n} = \frac{A_n}{Z}\frac{C_n}{r_S^{\,n}}\theta^{n/2} \tag{18}$$

where for the hexagonal structure, $Z = 6$. Setting eq 18 into eq 12, we obtain a fundamental formula for calculating the 2D spreading pressure $\varphi$ in the hexagonal-structure halide adlayer,

$$\varphi = \frac{1}{4a_S}\sum_n (n+2)\frac{A_nC_n}{r_S^{\,n}}\theta^{(n+4)/2} - \frac{kT}{a_S}\ln(1-\theta) \tag{19}$$

Similar to bulk matter, the two-dimensional compressibility $\kappa_{2D}$ is defined as[32]

$$\kappa_{2D} \equiv -\frac{1}{a}\left(\frac{\partial a}{\partial \varphi}\right)_T \tag{20}$$

and the area elasticity is the reciprocal of 2D isothermal compressibility[25,33]

$$\kappa_{2D}^{\,-1} = -a\frac{\mathrm{d}\varphi}{\mathrm{d}a} = \theta\frac{\mathrm{d}\varphi}{\mathrm{d}\theta} \tag{21}$$

From eq 12, $\kappa_{2D}^{-1}$ reads

$$\kappa_{2D}^{\,-1} = \frac{ZW\theta^2}{a_S} + \frac{2Z\theta^3}{a_S}\frac{\mathrm{d}W}{\mathrm{d}\theta} + \frac{kT\theta}{a_S(1-\theta)} + \frac{Z\theta^4}{2a_S}\frac{\mathrm{d}^2W}{\mathrm{d}\theta^2} \tag{22}$$

which show that the adsorbate density $\Gamma$ or $\theta$, as well as the adatom−adatom energy $W$ with its derivatives, determines the size of the 2D isothermal compressibility. Setting eq 18 into eq 22, we have

$$\kappa_{2D}^{\,-1} = \sum_n \frac{\sqrt{3}}{2}(n^2+6n+8)\frac{A_nC_n}{r_s^{\,n+2}}\theta^{(n+4)/2} + \frac{2kT}{\sqrt{3}r_S^{\,2}}\frac{\theta}{1-\theta} \tag{23}$$

which is the fundamental formula for calculating the 2D isothermal compressibility in the hexagonal-structure halide adlayer.

**2.3 Theoretical *θ*-*E* Relation.** Even though 2D spreading pressure and 2D isothermal compressibility in the adlayer are important, the coverage−potential ($\theta-E$) curves have been a most important concern of electrochemists[1−8,14]. In this subsection, the theoretical $\theta - E$ relation is established, based on the following thermodynamic formulas and the definition of the area elasticity eq 21.

On one hand, on the basis of thermodynamics,[16] we have

$$A\mathrm{d}\varphi = N_A\mathrm{d}\mu_{ad}, \quad \text{i.e.,} \quad a\mathrm{d}\varphi = \mathrm{d}\mu_{ad} \tag{24}$$

where $\mu_{ad}$ is chemical potential of the adsorbates. As to the relation between chemical potential $\mu_{ad}$ and electrode potential $E$, the essential electrode process may be considered as eq 1. At equilibrium, chemical potentials of the species on the left-handed side of eq 1 must be equal to those on the right side. Thus, the chemical potential of adsorbates $\mu_{ad}$ is

$$\mu_{ad} = \mu_{sol} - \gamma E \qquad \text{and} \qquad \mathrm{d}\mu_{ad} = \mathrm{d}\mu_{sol} - \gamma\mathrm{d}E \tag{25}$$

where $\mu_{sol}$ is chemical potential of the solution. According to thermodynamics[16]

$$\mathrm{d}\mu_{sol} = kT\,\mathrm{d}\ln C \tag{26}$$

where $C$ is the concentration of the halide. From eqs.(25) and (26),

$$\mathrm{d}\mu_{ad} = -\gamma\,\mathrm{d}E + kT\,\mathrm{d}\ln C \tag{27}$$

Putting eq 27 into 24, we obtain

$$a\,\mathrm{d}\varphi = -\gamma\,\mathrm{d}E + kT\,\mathrm{d}\ln C \tag{28}$$

On the other hand, from the definition of $k_{2D}^{-1}$ in eq 21, we have

$$a\,\mathrm{d}\varphi = -\kappa_{2D}^{\,-1}\,\mathrm{d}a \tag{29}$$

thus,

$$-\gamma\,\mathrm{d}E + kT\,\mathrm{d}\ln C = -\kappa_{2D}^{\,-1}\,\mathrm{d}a \tag{30}$$

By using $\theta = a_S/a$ in eq 30, we obtain a differential relation between the electrode potential $E$ and adsorbate coverage $\theta$

$$\mathrm{d}E = -\frac{a_S\,\kappa_{2D}^{\,-1}}{\gamma\theta^2}\,\mathrm{d}\theta + \frac{kT}{\gamma}\,\mathrm{d}\ln C \tag{31}$$

Setting eq 23 into eq 31 and integrating eq 31, we have obtained the fundamental theoretical relation between the coverage $\theta$ and electrode potential $E$ as follows

$$E = \sum_n \frac{-3}{2\gamma}(n+4)\frac{A_nC_n}{r_S^{\,n}}\theta^{(n+2)/2} - \frac{kT}{\gamma}\ln\frac{\theta}{1-\theta} + \frac{kT}{\gamma}\ln C + E_0 + \sum_n \frac{3}{2\gamma}(n+4)\frac{A_nC_n}{r_S^{\,n}}\theta_0^{\,(n+2)/2} + \frac{kT}{\gamma}\ln\frac{\theta_0}{1-\theta_0} - \frac{kT}{\gamma}\ln C_0 \tag{32}$$

where $E_0$, $C_0$, and $\theta_0$ are respectively the initial values of electrode potential and the concentration and coverage of the adlayer, which results from the integral constants in eq 31, fixed by one point in the experimental $\theta-E$ curves. Thus, the fundamental relation between the electrode potential $E$ and adsorbate coverage $\theta$ has been established.

## 3. Adsorbate−Adsorbate (Lateral) Interaction Energy

It is generally believed[34−37] that the lateral interaction of adsorbed particles on a solid surface is one of the most important factors which makes adsorption phenomena so varied and exciting. Indeed, it determines the formation of two-dimensional adsorbate structures, the phase transition in them, the coverage dependence of adsorption heat, kinetics of adsorption and surface diffusion, catalytic activity, etc. Our theoretical analysis in section 2 also shows that the 2D spreading pressure, 2D isothermal compressibility, and electrode potential versus coverage ($\theta-E$) curve in the adlayer are all dependent on the adsorbate−adsorbate interaction energy.

It is known[1−8,11,13] that adsorption of halide on Au(111) belongs to weak chemisorption. According to theory of chemisorption,[38−41] the components of the lateral interaction energies in the halide adlayer on Au(111) include: (i) The electrostatic energy among adions; (ii) Induction energy, i.e., induced dipole−induced dipole interaction energy due to the electrode potential; (iii) Lennard-Jones potential including the van der Waals attraction between two adatoms and Pauli repulsion; (iv) many-body interactions within the adlayer, such as the triple−dipole energy, and so on; (v) the substrate-mediated interaction energy. For most chemisorption systems, it is well-known[38−40,42] that the substrate-mediated interaction is dominant among the components in the lateral interaction energy, especially for most "small" atoms or molecules even at monolayer coverage.[43,44] Other components are rather small for the kinds of separation encountered in ordered chemisorption adlayers on surfaces. We consider and evaluate each as follows.

**3.1. Substrate-Mediated Interaction.** In the physisorption layer, the indirect lateral interaction is the substrate-mediated dispersion energy proposed by Sinanoglu, Pitzer, and McLachlan et al.[45,46] A quite drastic simplification expression of the Sinanoglu−Pitzer−McLachlan energy is[22,35]

$$S(r) = \frac{9}{16}\alpha\frac{1}{r^3}\left(\frac{S_3}{L^3}\right) \tag{33}$$

where $\alpha$ is the adatom polarizability, $S_3/L^3$ is the negative one-adatom holding potential, $S_3$ is the strength coefficient of adatom−substrate interactions, $L$ is the perpendicular distance of the adatom from the substrate, and 9/16 is an empirical parameter.[22,23,35] In the chemisorption adlayer, the indirect substrate-mediated interaction originates from a mutual coupling of the adatom valence shells via the substrate valence band, so-called, the indirect electronic interaction.[38−40,47,48] There are no analytical formulas for the description of the indirect electronic interaction.

The halide adatom on Au(111) is weakly chemisorbed because their chemisorption energies are quite smaller than the typical value of chemisorption energy of an adatom 1−7 eV.[40,47,49] For example, the adsorption of bromide on Au(111) is 120 kJ/mol (about 1.2 eV/mol) and iodide and chloride have the similar values with the sequences of increasing adsorbility: $Cl^- < Br^- < I^-$.[11,13] Many experimental results indicate[50,51] that the adatom−adatom interaction in halide adlayer on Au(111) is strongly repulsive in a wide range of the coverage $\theta$ and is not oscillatory in sign with the adatom−adatom distance. These facts give a hint that the form of indirect substrate-mediated interaction of halide on Au(111) approximate to that for a strong physisorption system as eq 33, which is proportional to $r^{-3}$. Additionally, Grimley[52] found that the asymptotic form of the indirect electronic interaction decays with $r^{-3}$. Hence for simplicity of the calculation, we attempt to use a simplification form of the Sinanoglu−Pitzer−McLachlan energy, such as eq 33, to express empirically the indirect electronic interaction in the halide adlayer because there no analytical formula for the indirect electronic interaction in the literature, i.e.,

$$W_{sub} = \frac{A_3}{6}\alpha\frac{1}{r^3}\left(\frac{S_3}{L^3}\right) \tag{34}$$

where the units are $W_{sub}$ in eV, $r$, $L$ in Å, and $\alpha$ in Å$^3$. The experimental values of Au−$X^-$ interlayer spacing ($2L$) in the halide adlayer have been used in eq 34. It is noteworthy that eq 34 is an empirical expression of the substrate-mediated interaction.

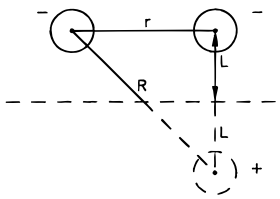


**Figure 2.** The coordinates for the electrostatic interaction between two adions.

**3.2. Electrostatic Interaction.** Many experimental results indicate[1−8,12,29,30,53,54] that halide ions (aq) undergo spontaneous oxidation and transfer charge to Au electrode upon chemisorption and form almost a zero valent halogen adlayer; the halide adsorbate on Au(111) can carry a rather small charge, $(-1-\gamma)e$[1−8,14].

Similar to Langmuir's treatment of Cs on W,[55] the ionic repulsion between an adsorbate and the dipole formed by the ion and its images is[56]

$$U_{repul} = \frac{(-1-\gamma)^2e^2}{\epsilon r} - \frac{(-1-\gamma)^2e^2}{\epsilon R} \tag{35}$$

where $\epsilon$ is the dielectric constant in the adlayer. The coordinate of interacting two adions are shown in Figure 2. From Figure 2, we see

$$R^2 = (2L)^2 + r^2 \tag{36}$$

and

$$\frac{1}{R} = [r^2 + (2L)^2]^{-1/2} \approx \frac{1}{r} - \frac{2L^2}{r^3} + \frac{6L^4}{r^5} - \frac{20L^6}{r^7} + \frac{70L^8}{r^9} \tag{37}$$

where we take the first five terms of the binomial expansion. After inserting eq 37 into 35 and taking the lattice sums, the electrostatic interaction energy between adions is

$$W_{el} = \frac{14.4(1+\gamma)^2}{6\epsilon}\left(\frac{2A_3L^2}{r^3} - \frac{6A_5L^4}{r^5} + \frac{20A_7L^6}{r^7} - \frac{70A_9L^8}{r^9}\right) \tag{38}$$

where the units are $W_{el}$ in eV, $L$ and $r$ in Å.

**3.3. Induction Interaction Energy.** Induction interaction energies in the adlayer are rather small like those between molecules in the solid.[58] The induced dipole of an adatom on Au(111) produced by the electrode potential is approximately[58]

$$\mu_0 = \mu_0^{\,0} + \alpha F = \mu_0^{\,0} + \frac{1}{3}\frac{\alpha E'}{L} \tag{39}$$

where $F$ is the electric field at an adsorbate and $\mu_0^0$ is the dipole moment when the electrode potential $E'$ referenced to a Ag/AgCl electrode is 0. $\alpha$ is the polarizability of an adatom. The units in eq 39 are $\mu_0$, $\mu_0^0$ in debye, $E'$ in V, $L$ in Å, and $\alpha$ in Å$^3$. After taking the lattice sums, we obtain the induced dipole−induced dipole interaction energy

$$W_{ind} = 0.104\frac{A_3\mu_0^{\,2}}{r^3} \tag{40}$$

where the units are $W_{ind}$ in eV, $r$ in Å. Because the induced dipole $\mu_0$ of halide adsorbate on Au(111) is rather small, we have omitted the image field effect of the substrate and depolarization effect between adatoms.[57] In addition, we have disregarded the induction interaction energy between the halide

adatoms on Au(111) induced by the ionic charge $(-1-\gamma)e$ of the adatoms, because the charge $(-1-\gamma)e$ of the adatoms is small and usually the induction energy between molecules is rather small.[58]

**3.4. Lennard-Jones Potential.** We combine Pauli repulsion between adatoms from the wave function overlap of the closed shells and van der Waals attraction between adatoms into the Lennard-Jones (12,6) potential,

$$U_{L-J} = \epsilon\left[\left(\frac{r_0}{r}\right)^{12} - 2\left(\frac{r_0}{r}\right)^{6}\right] \tag{41}$$

where $\epsilon$ is the depth of the potential energy minimum, $r_0$ is the van der Waals diameter of the adsorbate atoms. After taking the lattice sums, the Lennard-Jones potential (12,6) is

$$W_{L-J} = 8.625 \times 10^{-5}\,\epsilon\left[\frac{A_{12}}{6}\left(\frac{r_0}{r}\right)^{12} - \frac{A_6}{3}\left(\frac{r_0}{r}\right)^{6}\right] \tag{42}$$

where the unit are $W_{L-J}$ in eV, $r_0$ in Å, $\epsilon$ in K.

**3.5. Nonadditive Three Body Potential.** The contribution of the nonadditive three body potential is present in the adlayer. We estimate it by using the form of the Axilrod−Teller−Muto triple dipole interaction among the adatoms[23,24,35]

$$W_{thr} = \frac{A_9}{6}\frac{\upsilon}{3r^9} \tag{43}$$

where $\upsilon$ is strength of the three body interaction. The units are $W_{thr}$ in eV, $\upsilon$ in eV Å$^9$.

Summing the foregoing components of the lateral interaction in the adlayer from eqs 34, 38, 40, 42, and 43, we get the coefficient $C_n$, where $n = 3, 5, 6, 7, 9, 12$, in the effective pair interaction $W$ between the adsorbates in eq 18,

$$C_3 = \frac{4.8(1+\gamma)^2 L^2}{\epsilon} + 0.104\,\mu_0{}^2 + \frac{\alpha S_3}{6L^3}$$

$$C_5 = -\frac{14.4(1+\gamma)^2 L^4}{\epsilon}$$

$$C_6 = -2.875 \times 10^{-5}\,\epsilon\, r_0{}^6$$

$$C_7 = \frac{48(1+\gamma)^2 L^6}{\epsilon}$$

$$C_9 = -\frac{168(1+\gamma)^2 L^8}{\epsilon} + 5.556 \times 10^{-2}\,\upsilon$$

$$C_{12} = 1.438 \times 10^{-5}\,\epsilon\, r_0{}^{12} \tag{44}$$

Thus, from eqs 16, 18, 19, 23, 32, and 44, we have calculated the total lateral interaction energy, 2D spreading pressure, 2D isothermal compressibility, and the potential−coverage curve with the parameters in Table 1.

In Table 1, the Au−X interlayer spacing ($2L$) of the halide adlayer are the experimental values in refs 7 and , except that of the iodide adlayer when $\theta \le 0.35$, which can be calculated as follows. The Au−I interlayer spacing can be estimated theoretically in terms of the covalent bonding radius 1.33 Å of iodine and the atomic radius 1.44 Å of gold.[7] When $\theta \le 0.35$, the iodine adatoms are assumed to be at the "hollow" sites and the Au−I interlayer spacing is 2.21 Å, thus $L = 1.10$ Å. The values of electrosorption valency $\gamma$ are chosen as the experimental ones,[7,8,12,54,64] which for chloride, bromide, and iodide adlayer in the hexagonal phase are −0.7, −0.8, and −1.0, respectively, and for iodide adlayer in the $(p\times\sqrt{3})$ phase is −0.7. The $\gamma$ for iodide in the $\theta \le 0.35$ phase is chosen as −0.4 according to its changing tendency in experiments and the experimental value of $\gamma_{Br}$ in a similar case,[30] because we did not find it in literature. The Au−Au atomic nn distance $r_S = 2.885$ Å[7,8] and the temperature is assumed as 298 K. The polarizabilities and dielectric constants are those of the halogen atoms. The electrode potentials $E'$ in the induced dipole moment $\mu_0$ are from the average experimental values. For lack of parameters $S_3$, $\epsilon$, $\upsilon$, $\mu_0{}^0$ for $Cl^-$, $Br^-$, and $I^-$ adions, we estimate them by using the parameters of Ar, Kr, and Xe atoms, respectively, because the halide ions and the corresponding atoms of noble gases have nearly the same electronic structure and atomic volume, and also, $S_3$ is an empirical parameter.

## 4. Results and Discussion

**4.1. Theoretical $\theta$−E Curve.** The theoretical coverage-($\theta$)−potential($E$) curves of the iodide, bromide and chloride adlayer on Au(111) are calculated with eqs 32, 16, and 44 and shown in Figures 3, 4, and 5, respectively, where the experiment data points are also dotted. The theoretical curves agree quite well with the experimental ones.[7,8] Also, at the phase transition point in the 0.1 M iodide adlayer, the calculated potential $E$ at $\theta = 0.409$ in the $(p\times\sqrt{3})$ centered rectangular structure is found to be equal to that at $\theta = 0.415$ in the hexagonal structure (Figure 3) which is associated with the experiments.[7] The theoretical $\theta$−E curve in the $\theta \le 0.35$ phase is obtained in the curve (III) of Figure 3 and is also in accordance with the tendency of the experiments.[14,65]

**4.2. 2D Isothermal Compressibility.** The 2D isothermal compressibility in the three halide adlayers on Au(111) is calculated by using eqs 23, 44, and 16 and is given in Table 2. The experiment values $\kappa_M$ in the tables are estimated from the data in refs 7 and 8 by using Toney et al.'s method.[9,10] It can be seen that the calculated 2D isothermal compressibility $\kappa_{theory}$ is associated with the experimental measurement $\kappa_M$, which also indicates that our theory is in principle correct.

**4.3. The Lateral Interaction Energy.** The lateral interaction energy and their components in the halide adlayer on Au(111) are calculated and shown in Table 3. In the calculation, eqs 16, 18, and 44 were used for hexagonal structure, eqs. A-3 and A-4, in the Supporting Information and eq 44 were used for the $(p\times\sqrt{3})$ centered-rectangular structure. The results in Table 3 show that the calculated total lateral energy between halogen adatoms is strongly repulsive, which corresponds to the relative experiments for halides on metals.[3,50,53] For halogen chemisorbed on metal surfaces,[50,51] strong adatom−adatom repulsive interaction is indicated not only by the formation of two-dimensional adlayer structure, patterns of which show that it is repulsive,[27] but also by the core level binding energy shifts with increasing coverage for iodine on Fe(100), Ag(111), Cu(111), Cu(100), Ni(100), and Pt(111).[51] Ocko et al.'s experiments and theoretical results on the structure and phase behavior of electrodeposited halides on single-crystal metal surfaces[66,67] clearly demonstrated this lateral repulsive interaction. In fact, this strong adatom−adatom repulsive interaction often appears in chemisorption systems. As Zhdanov pointed out,[43] while the lateral interaction of physically adsorbed particles is attractive, in the case of chemisorption, the lateral interaction between nearest-neighbor adsorbed particles is, as a rule, repulsive. This repulsive interaction can be expected from a simple tight-binding scheme.[21b] The most excellent

**TABLE 1: Parameters Used in the Calculation of Halides on Au(111) Surface**

| parameter | chloride | bromide | iodide |
|---|---|---|---|
| $S_3$ (eV Å$^3$)[a] | 1.847 | 2.589 | 3.794 |
| $\alpha$ (Å$^3$)[b] | 2.21 | 3.31 | 5.29 |
| 2L (Å)[c] | 2.40 | 2.40 | 2.21($\theta \leq 0.35$) 2.30(rect) 2.40(hex) |
| $\epsilon$[d] | 2.10(−50 °C) | 3.09(20 °C) | 4.00 |
| $\gamma$[e] | −0.7 | −0.8 | −0.4($\theta \leq 0.35$) −0.7(rect) −1.0(hex) |
| $E'_{Ag/AgCl}$ (V)[f] | 0.73 | 0.6 | −0.6($\theta \leq 0.35$) −0.06(rect) 0.21(hex) |
| $\mu_0^0$ (Debye)[g] | 0.2 | 0.2 | 0.2 |
| $r_0$ (Å)[h] | 3.80 | 4.00 | 4.24 |
| $\in$ (K)[i] | 142.1 | 201.9 | 281.0 |
| $\upsilon$ (evÅ$^9$)[j] | 479 ± 11 | 1422 ± 33 | 462 ± 3 |

[a] Strength coefficient of adsorbate−substrate interactions from ref 35. [b] Polarizabilities from ref 59. [c] Au−halide interlayer spacing from refs 7 and 8. [d] Dielectric constant from ref 60. [e] Electrosorption valency (see section 3). [f] The electrode potential in eq 39 from refs 7 and 8. [g] The dipole moment from ref 23. [h] van der Waals diameter from ref 61. [i] L-J potential depth from ref 62. [j] Three-body interaction strength from ref 63.

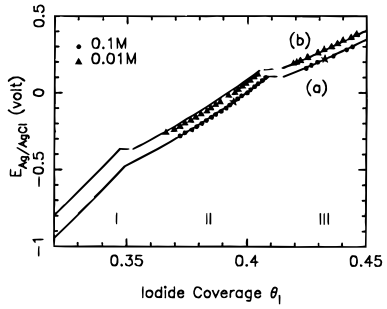


**Figure 3.** Theoretical potential ($E$)−coverage ($\theta$) curve in the iodide adlayer at various anion concentration and various phases in the electrolyte (a) 0.1 M, (b) 0.01M; (I) the $\theta \leq 0.35$ phase, (II) the $(p\times\sqrt{3})$ centered rectangular phase, (III) the hexagonal phase. The experimental points were obtained from Figure 4 and Figure 8b in ref 7 and shown with filled circles and triangles representing respectively 0.1 and 0.01 M iodide. The stars denote the initial values used in the calculation.

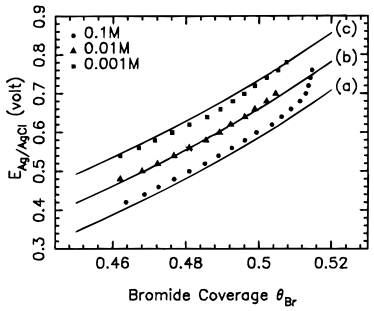


**Figure 4.** Theoretical potential ($E$)−coverage ($\theta$) curve in the bromide adlayer at various anion concentration in the electrolyte (a) 0.1 M, (b) 0.01 M, (c) 0.001 M. Theoretical points were obtained from Figure 3b in ref 8 and shown with filled circles, triangles, and squares representing respectively 0.1, 0.01, and 0.001 M bromide. The star denotes the initial values used in the calculation.

example of this repulsive interaction system has been given by Al-Sarraf and King's experiment.[68] They reported first direct measurement of adatom−adatom interaction energy for O/Ni(100) system and found that oxygen adatoms at next-nearest neighbor separations (3.52 Å) experience a relatively high mutual repulsive interaction energy, 33 kJ mol$^{-1}$, accurate to within a factor of 3, and that the nearest-neighbor repulsion is so high that nearest neighbor sites are never occupied in the established adlayer. Also for CO on Pd(100),[63,69] CO−CO interaction is dominated by repulsion interaction between the nearest neighbors which is about 0.35 eV/molecule.

The dominant component of the lateral energy in the halide adlayer on Au(111) is the substrate-mediated interaction, the calculated value of which in Table 3 agrees with the order of the magnitude of the indirect electronics interaction for the other

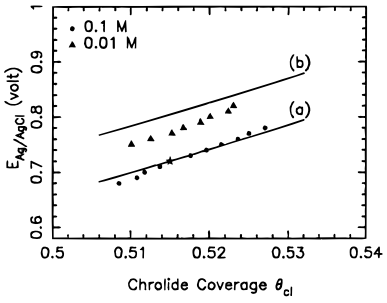


**Figure 5.** Theoretical potential ($E$)−coverage ($\theta$) curve in the chloride adlayer at various anion concentration in the electrolyte (a) 0.1 M, (b) 0.01M. Experimental data points were obtained from Figure 3a in ref 8 and shown with filled circles and triangles representing, respectively, 0.1 and 0.01 M chloride. The star denotes the initial values used in the calculation.

**TABLE 2: 2D Isothermal Compressibility in the Halide Adlayers on Au(111) (in Å$^2$/eV)**

(a) in the Iodide Adlayer

| | $\theta$ | | | | | |
|---|---|---|---|---|---|---|
| | 0.36 | 0.40 | 0.409 | 0.415 | 0.43 | 0.45 |
| $\kappa_{theory}$ | 8.27 | 5.37 | 4.85 | 6.06 | 5.20 | 4.23 |
| $\kappa_M$ | 7.47 | 6.05 | 5.79 | 5.90 | 5.50 | 5.02 |

(b) in the Bromide Adlayer

| | $\theta$ | | | |
|---|---|---|---|---|
| | 0.45 | 0.48 | 0.50 | 0.52 |
| $\kappa_{theory}$ | 8.99 | 6.81 | 5.63 | 4.63 |
| $\kappa_M$ | 9.46 | 8.32 | 7.66 | 7.09 |

(c) in the Chloride Adlayer

| | $\theta$ | | | |
|---|---|---|---|---|
| | 0.50 | 0.51 | 0.52 | 0.53 |
| $\kappa_{theory}$ | 8.57 | 7.93 | 7.33 | 6.77 |
| $\kappa_M$ | 7.16 | 6.88 | 6.62 | 6.37 |

chemisorption systems,[38−40] for example, CO on Pt(111).[27,42] The Lennard-Jones potential is also important, so is the electrostatic interaction when the absolute value of electrosorption valency is small.

The foregoing results indicate that the adatom−adatom interactions, especially repulsive interactions, in all the three halide adlayer on Au(111), cause continuous compression of the unit cell in the halide adlayer with an increase in the electrode potential and the adsorbate coverage and dominantly determine the structure and phase behavior. The calculated 2D spreading pressure $\varphi$, given in Table S1 in the Supporting Information, which increases with the increasing coverage $\theta$

**TABLE 3: Components of the Lateral Interaction Energy in the Halide Adlayer on Au(111) (in eV)**

(a) in the Iodide Adlayer

| | $\theta$ | | | | | |
|---|---|---|---|---|---|---|
| | 0.30 | 0.33 | 0.37 | 0.409 | 0.415 | 0.45 |
| $W_{sub}$ | 0.18875 | 0.21776 | 0.22579 | 0.26346 | 0.23654 | 0.26709 |
| $W_{el}$ | 0.03645 | 0.04901 | 0.01329 | 0.01533 | 0 | 0 |
| $W_{L-J}$ | −0.01222 | −0.01547 | −0.01990 | −0.02309 | −0.02451 | −0.02683 |
| $W_{ind}$ | 0.00453 | 0.00523 | 0.00025 | 0.00030 | 0.00329 | 0.00371 |
| $W_{thr}$ | 0.00005 | 0.00008 | 0.00013 | 0.00022 | 0.00022 | 0.00031 |
| $W_{total}$ | 0.21756 | 0.24931 | 0.21956 | 0.25622 | 0.21554 | 0.24428 |

(b) in the Bromide Adlayer

| | $\theta$ | | | |
|---|---|---|---|---|
| | 0.46 | 0.48 | 0.50 | 0.52 |
| $W_{sub}$ | 0.11786 | 0.12563 | 0.13357 | 0.14166 |
| $W_{el}$ | 0.01121 | 0.01189 | 0.01258 | 0.01327 |
| $W_{L-J}$ | −0.01725 | −0.01831 | −0.01911 | −0.01957 |
| $W_{ind}$ | 0.00838 | 0.00893 | 0.00950 | 0.01007 |
| $W_{thr}$ | 0.00105 | 0.00127 | 0.00153 | 0.00182 |
| $W_{total}$ | 0.12125 | 0.12941 | 0.13807 | 0.14725 |

(c) in the Chloride Adlayer

| | $\theta$ | | | |
|---|---|---|---|---|
| | 0.500 | 0.510 | 0.520 | 0.530 |
| $W_{sub}$ | 0.06362 | 0.06554 | 0.06748 | 0.06943 |
| $W_{el}$ | 0.04164 | 0.04278 | 0.04393 | 0.04509 |
| $W_{L-J}$ | −0.01177 | −0.01215 | −0.01251 | −0.01283 |
| $W_{ind}$ | 0.00706 | 0.00727 | 0.00749 | 0.00771 |
| $W_{thr}$ | 0.00051 | 0.00056 | 0.00061 | 0.00067 |
| $W_{total}$ | 0.10106 | 0.10400 | 0.10700 | 0.11007 |

and makes continuous compression in halide adlayers, further support this point of view.

**4.4. Discussion.** In this paper, a simple Bragg−Williams approximation is used, which is usually used to handle adsorption of molecules on metal electrode.[17,18] Price and Venables[22] pointed out that as $\theta \cong 1$, the Bragg−Williams approximation becomes equivalent to assuming a random distribution of a small number of noninteracting vacancies. This approximation is good and much better than the normal application to regions of low coverage. With this approximation, we have achieved satisfactory results in the halide adlayers on gold surface. However, for an incommensurate close-packed monolayer, the increase of coverage with increasing potential results from a uniform compression of the adlayer lattice, i.e., a collective lateral motion of the adsorbates occurs during electrocompression. This uniform compression model is also reasonable. The difference between the two models is that the former takes the configuration entropy effect into account while the latter does not. Here the contribution from configuration entropy to thermodynamic quantities, such as chemical potential et al., is estimated as follows.

Taking $I^-$ on Au(111) as an example, we can obtain expression of chemical potential from eq 2,

$$\mu = kT \ln \frac{\theta}{1-\theta} + (U - kT \ln j^{(S)}(T)) + \left(ZW\theta + \frac{Z\theta^2}{2}\frac{dW}{d\theta}\right) \quad (45)$$

which is similar to eqs 14−46 in ref 17a. From the deducing process, we know that the first term in eq 45 is the contribution of configuration entropy (see eq 7−11 in ref 17b). The second term, where $U$ is the adsorption energy per atom, does not change with the changing of coverage $\theta$. The last term is the contribution from intermolecular interaction energy. The ratio $\eta_\mu$ of the contribution from the configuration entropy (the first term) to the chemical potential is

$$\nu_\mu = \left|\frac{kT \ln \frac{\theta}{1-\theta}}{\mu}\right| \le \left|\frac{kT \ln \frac{\theta}{1-\theta}}{ZW\theta}\right| = \left|\frac{0.0043\ \text{eV}}{W}\frac{\ln\frac{\theta}{1-\theta}}{\theta}\right| \quad (46)$$

In the experimental condition,[7] $\theta = 0.36 \sim 0.45$ and the calculated $W = 0.22 \sim 0.24$ eV; putting them into eq 46, we find $\theta = 0.36$, $\eta_\mu \le 3.0\%$, and $\theta = 0.45$, $\eta_\mu \le 0.8\%$. Thus, the contribution from configuration entropy to the chemical potential at high coverage is calculated to be small. From the two $\eta_\mu$ values and eq 25, the contribution of the configuration entropy term to the calculation of $\theta - E$ curves is also calculated to be small. Similarly, we have calculated the contribution of the configuration entropy to the spreading pressure and the 2D isothermal compressibility, and the same conclusions are obtained as $\theta = 0.36$, $\eta_\varphi \approx 5.4\%$, $\eta_{\kappa_{2D}^{-1}} = 1.8\%$; and $\theta = 0.45$, $\eta_\varphi = 3.9\%$, $\eta_{\kappa_{2D}^{-1}} = 2.1\%$.

The forgoing results indicate that, for an incommensurate close-packed monolayer such as an $I^-$/Au(111) system, the uniform compression model, and the Bragg−Williams approximation have nearly the same results. Nevertheless, in the low coverage and phase transition region, the contribution from configuration entropy can be significant.

## 5. Conclusion

A simple physical model and fundamental statistical mechanics formulas of electrocompression in electrodeposited halide monolayer on Au(111) are established. The lateral interaction energy, 2D isothermal compressibility and coverage−potential curves in the halide adlayer on Au(111) surface are computed, which agrees well with the experiments. The results indicate that the lateral interaction energy (especially the adatom−adatom repulsive interactions) and the adsorbate density determine the size of the compressibility in the halide adlayer on Au(111) with increasing the electrode potential. Also, the electrosorption valency of the halide adlayer plays an important role.

**Acknowledgment.** We are most grateful to Professor M. J. Weaver and Dr. Xiaoping Gao for recommending this interesting topic and for their helpful discussions. Without their help this work could not have been accomplished. We also express our heartfelt thanks to the referees for their helpful and constructive comments. This work was in part supported by the National Science Foundation of China.

**Supporting Information Available:** Table 1S listing the calculated data of two-dimensional (2D) spreading pressure in the iodide, bromide, and chloride adlayer on Au(111); the appendix presenting of the fundamental thermodynamical formulas for the effective pair interaction energy, 2D spreading pressure, isothermal compressibility, and potential−coverage relation in the $(p\times\sqrt{3})$ centered rectangular halide adlayer on Au(111) (3 pages). Ordering information is given on any current masthead page.

## References and Notes

(1) Gao, X.; Hamelin, A.; Weaver, M. J. *J. Chem. Phys.* **1991**, *95*, 6993.
(2) Gao, X.; Weaver, M. J. *J. Am. Chem. Soc.* **1991**, *114*, 8544.
(3) Tao, N. J.; Lindsay, S. M. *J. Phys. Chem.* **1992**, *96*, 5213.
(4) Gao, X.; Edens, G. J.; Liu, F.-C.; Hamelin, A.; Weaver, M. J. *J. Phys. Chem.* **1994**, *98*, 8086.
(5) Magnussen, O. M.; Ocko, B. M.; Wang, J. X.; Adzic, R. R. *J. Phys. Chem.* **1996**, *100*, 5500.

(6) Wang, J.; Watson, G. M.; Ocko, B. M. *Phys. A* **1993**, *200*, 679.
(7) Ocko, B. M.; Watson, G. M.; Wang, J. *J. Phys. Chem.* **1994**, *98*, 897.
(8) Magnussen, O. M.; Ocko, B. M.; Adzic, R. R.; Wang, J. X. *Phys. Rev. B* **1996**, *51*, 5510.
(9) Toney, M. F.; Gordon, J. G.; Samant, M. G.; Borge, G. L.; Melroy, O. R. *Phys. Rev. B* **1992**, *45*, 9362.
(10) Toney, M. F.; Samant, M. G.; Borge, G. L.; Wiesler, D. G.; Yee, D.; Sorensen, L. B. *Langmiur* **1991**, *7*, 796.
(11) Schultze, J. W.; Vetter, K. J. *J. Electroanal. Chem.* **1973**, *44*, 63.
(12) Meakin, M. R.; Li, T. T.; Melroy, O. R. *J. Electroanal. Chem.* **1988**, *243*, 343.
(13) Anson, F. C. *Acc. Chem. Res.* **1975**, *8*, 400.
(14) Weaver, M. J.; Gao, X. *Annu. Rev. Phys. Chem.* **1993**, *44*, 459.
(15) Hofmann F.; Toennies J. P. *Chem. Rev.* **1996**, *96*, 1307.
(16) Fowler, R.; Guggenheim, E. A. *Statistical Thermodynamics*; University Press: Cambridge, 1956.
(17) Hill, T. L. *An Introduction to Statistical Thermodynamics*; Addison-Wesley: Reading, 1960. (a) Chapter 14, (b) Chapter 7, (c) Chapter 2.
(18) Guidelli, R. In *Adsorption of Molecules at Metal Electrodes*; Lipkowski, J.; Ross P. N., Eds.; VCH: New York; 1992; Chapter 1.
(19) Ponec, V.; Knor, Z.; Cerny, S. *Adsorption on Solids*; Butterworths: London, 1974; 333.
(20) Adamson, A. W. *Physical Chemistry of Surfaces*, 4th ed.; Wiley: New York, 1982.
(21) Desjonqueres, M. C.; Spanjarrd, D. *Concepts in Surface Physics*; Springer: Berlin, 1993. (a) section 6.5, (b) 490−492.
(22) Price, G. L.; Venables, J. A. *Surf. Sci.* **1976**, *59*, 509.
(23) Bruch, L. W.; Cohen, P. I.; Webb, M. B. *Surf. Sci.* **1976**, *59*, 1.
(24) Bruch, L. W.; Philips, J. M. *Surf. Sci.* **1980**, *91*, 1.
(25) Shaw, C. G.; Fain, S. C., Jr. *Surf. Sci.* **1979**, *83*, 1.
(26) Unguris, J.; Bruch, L. W.; Moog, E. R.; Webb, M. B. *Surf. Sci.* **1981**, *109*, 522.
(27) Persson, B. N. J. *Surf. Sci. Rept.* **1992**, *15*, 1.
(28) Sellers, H. *J. Phys. Chem.* **1994**, *98*, 968.
(29) Gao, P.; Weaver, M. J. *J. Phys. Chem.* **1986**, *90*, 4057.
(30) Van Huong, C. N.; Hinnen, C.; Rouseau, A. *J. Electroanal. Chem.* **1983**, *151*, 149.
(31) Zuker, I. J. *J. Math. Phys.* **1974**, *15*, 187.
(32) Dash, J. G. *Films on Solid Surfaces*; Academic Press: New York, 1975; 169.
(33) Partington, J. R. *An Advanced Treatise on Physical Chemistry*; Longmans: London, 1949; Vol. 1, Page 820.
(34) Naumovets, A. G. *Surf. Sci.* **1994**, *299/300*, 709.
(35) Bruch, L. W. *Surf. Sci.* **1983**, *125*, 194.
(36) Joos, B.; Ren, Q.; Duesbery, M. S. *Surf. Sci.* **1994**, *302*, 385.
(37) Bertel, E.; Netzer, F. P. *Surf. Sci.* **1980**, *97*, 409.
(38) Muscat, J.-P. *Prog. Surf. Sci.* **1987**, *25*, 211.
(39) Muscat, J.-P.; Newns, D. M. *Prog. Surf. Sci.* **1978**, *9*, 1.
(40) Einstein, T. L. In *Chemistry and Physics of Solid Surfaces*; Vanselow, R., Ed.; CRC Press: Boca Raton, 1979; Vol. 2, 181.
(41) Lombardo, S. J.; Bell, A. T. *Surf. Sci. Rept.* **1991**, *13*, 1.
(42) Schweizer, E.; Persson, B. N. J.; Tushaus, M.; Hoge, D.; Bradshaw, A. M. *Surf. Sci.* **1989**, *213*, 49.
(43) Zhdanov, V. P. *Elementary Physicochemical Processes on Solid Surfaces*; Plenum: New York, 1991; p 105.
(44) N*φ*rskov, J. K. In *Chemistry Physics of Solid Surface*; King, D. A., Ed.; Elsevier: Amsterdam, 1993; Vol. 6, Chapter 1.
(45) Sinanoglu, O.; Pitzer, K. S. *J. Chem. Phys.* **1960**, *32*, 1279.
(46) McLachlan, A. D. *Mol. Phys.* **1964**, *7*, 381.
(47) Gomer, R. *Acc. Chem. Res.* **1975**, *8*, 420.
(48) Steele, W. *Chem. Revs.* **1993**, *93*, 2355.
(49) Einstein, T. L.; Schrieffer, J. R. *Phys. Rev. B* **1973**, *7*, 3629.
(50) Dowben, P. A. *CRC Critical Revs. Solid States Mater. Sci.* **1987**, *13*, 191.
(51) Somerton, C.; McConville, C. F.; Woodruff, D. P.; Jones, R. G. *Surf. Sci.* **1984**, *136*, 23.
(52) Grimley, T. B. *Proc. Phys. Soc. London* **1967**, *90*, 751.
(53) Soriaga, P.; Stickney, J. L. *J. Phys. Chem.* **1991**, *95*, 5245.
(54) Sedlmaier, H. D.; Plieth, W. J. *J. Electroanal. Chem.* **1984**, *180*, 219.
(55) Langmuir, I. *J. Am. Chem. Soc.* **1932**, *54*, 2798.
(56) Bockris, J. OM.; Devanathan, M. A. V.; Muller, K. *Proc. R. Soc. London A* **1963**, *274*, 55.
(57) Buckingham, A. D.; Galwas, P. A.; Liu, F-C. *J. Mol. Struct.* **1983**, *100*, 3.
(58) Buckingham, A. D. In *Intermolecular Forces: From Diatomics to Biopolymers*; Pullman, B., Ed.; Wiley: New York, 1978; Chapter 1.
(59) Huyskens, P. L.; Luck, W. A. P.; Zeegers-Huyskens, T. *Intermolecular Forces*; Springer: Berlin, 1991; Table 4.
(60) Weast, R. C., Ed. *CRC Handbook of Chemistry and Physics* 71st ed.; CRC Press: Boca Raton, 1990−1991.
(61) Bondi, A. *J. Phys. Chem.* **1964**, *68*, 441.
(62) Baker, J. A. In *Rare Gas Solids*; Klein, M. L., Venables, J. A., Eds.; Academic Press: New York, 1976; Vol. 1, Chapter 4.
(63) Tracy, J. C.; Palmberg, P. W. *J. Chem. Phys.* **1969**, *51*, 4852.
(64) Rath, D. L.; Hansen, W. N. *Surf. Sci.* **1984**, *136*, 195.
(65) Wandlowski, Th.; Wang, J. X.; Magnussen, O. M.; Ocko, B. M. *J. Phys. Chem.* **1996**, *100*, 10277.
(66) Ocko, B. M.; Wandlowski, Th. In *Proceedings of the Materials Research Society*: *Electrochemical Synthesis and Modification of Materials*; Delplancke, J.; Corcoran, S.; Moffat, T., Eds.; BNL-64433; November, 1996; p 1-13.
(67) Ocko, B. M.; Wang, J. X.; Wandlowski, Th. *Phys. Rev. Lett.* **1997**, *79*, 1511.
(68) Al-Sarraf, N.; King, D. A. *Surf. Sci.* **1994**, *307/309*, 1.
(69) Ertl, G. *J. Vac. Sci. Technol.* **1977**, *14*, 435.
(70) Kittle, C. *Introduction to Solid-State Physics*, 5th ed.; Wiley: New York, 1976; Chapter 5.